ELSEVIER

Journal of Molecular Catalysis A: Chemical 169 (2001) 105–112

JOURNAL OF MOLECULAR CATALYSIS A: CHEMICAL

www.elsevier.com/locate/molcata

Characterization of Cr^{2+} and ethylene polymerization on Cr/SiO_2 catalysts

Alexandre B. Gaspar, Ruth L. Martins, Martin Schmal, Lídia C. Dieguez*

NUCAT-PEQ-COPPE, Universidade Federal do Rio de Janeiro C.P. 68502, CEP 21945-970 Rio de Janeiro, Brazil

Received 27 April 2000; accepted 11 October 2000

Abstract

Cr/SiO_2 catalysts were prepared by impregnation of chromium acetate (1 and 3 wt.% Cr) and bis(triphenylsilyl)chromate (0.5 wt.% Cr) over commercial silica. These samples were analyzed by temperature programmed reduction (TPR) and infrared spectroscopy (FT-IR) of CO and C_2H_4 adsorbed in order to characterize the chromium species, mainly Cr^{2+} species distribution ($Cr^{2+}{}_A$, $Cr^{2+}{}_B$ and $Cr^{2+}{}_C$) and polymerization aspects. The catalysts prepared with chromium acetate presented only Cr^{6+} after calcination, while the catalyst prepared with bis(triphenylsilyl)chromate presented Cr^{6+} and a fraction of Cr^{3+}. After reduction with CO, the catalysts prepared with chromium acetate showed more $Cr^{2+}{}_B$ than $Cr^{2+}{}_A$ species. The distribution of Cr^{2+} species influenced the catalytic activity. The catalyst with 3 wt.% Cr from acetate presented the greatest amount of species $Cr^{2+}{}_A$ and $Cr^{2+}{}_B$ and the best polymerization activity. The behavior of isolated hydroxyls band during polymerization tests, characterized by FT-IR, suggests its participation in the reaction mechanism.

Keywords: Cr/SiO_2; TPR; FT-IR; Ethylene polymerization

1. Introduction

Cr/SiO_2 catalysts have been used in the ethylene polymerization since 1950s decade. Despite the efforts of many researchers, some parameters of this system, like the distribution of active sites to polymerization, still remain not well characterized. Nowadays, there is a general agreement to ascribe the Cr^{2+} species as the active site to ethylene polymerization. The formation of three different Cr^{2+} species has been observed as a function of the chromium-surface hydroxyl interaction [1–6]. These species are assigned as $Cr^{2+}{}_A$, $Cr^{2+}{}_B$ and $Cr^{2+}{}_C$. $Cr^{2+}{}_A$ is the the most reactive species involved in the polymerization [4,6]. The $Cr^{2+}{}_A$ and $Cr^{2+}{}_B$ species can be identified by infrared spectroscopy (FT-IR) of carbon monoxide adsorbed at 2179 and 2188 cm^{-1}, respectively, while $Cr^{2+}{}_C$ can be seen in the hydroxyl group region at 3600 cm^{-1} [2]. The amount of each species depends on the calcination temperature, as well as other preparation parameters. $Cr^{2+}{}_B$ and $Cr^{2+}{}_C$ species decrease with increase of this temperature, following by the reduction on the surface hydroxyls and the appearance of inactive Cr^{3+} from Cr^{6+} decomposition. On the other hand, $Cr^{2+}{}_A$ is transformed into $Cr^{2+}{}_C$ at high temperatures (973 K) under vacuum [4,6]. These changes in the chromium species distribution modify the polymerization activity.

Several polymerization mechanisms have been reported [6–13], with two different reaction pathways.

* Corresponding author. Fax: +55-21-590-7135.
E-mail address: lidia@peq.coppe.ufrj.br (L.C. Dieguez).

1381-1169/01/$ – see front matter
PII: S1381-1169(00)00481-7

Jozwiak et al. [7] and Groeneveld et al. [8] suggested that initiation step starts with the migration of a proton from the hydroxyls adjacent to the active site to the monomer. They also suggested that the initiation proceeds via the adsorption of ethylene on the active Cr site and then its combination with an adjacent hydroxyl yielding an ethyl group. However, McDaniel and Welch [9,10] reported that high activity could be obtained by using completely dehydroxilated catalysts. Other mechanisms were proposed, without hydrogen transfer. Kantcheva et al. [11] suggested a mechanism via carbene ion, where ethylene is adsorbed directly on Cr sites with the formation of ethylidene (Cr=CH–R) species, preceding the formation of polymer chains. Ghiotti et al. [6] proposed the formation of a metallocyclobutane structure obtained by adsorption of two ethylene molecules on active Cr site. They also observed a band at 2750 cm^{-1} corresponding to the υ(C–H) mode of a carbene group interacting with the Cr site. Thus, there are different possibilities of mechanisms taking place, but the prevailing mechanism will depend on the surface active Cr sites and their vicinity.

The distribution of Cr^{2+} species and the polymerization activity of the Cr/SiO_2 catalysts have been determined in the literature by infrared spectroscopy (FT-IR) of CO and C_2H_4 adsorbed, although these analyses have been reported separately. Thus, the aim of this work is to determine the Cr^{2+} species distribution and its behavior in the ethylene polymerization activity on Cr/SiO_2 catalysts with different chromium contents and precursor salts. Analyses of temperature programmed reduction (TPR) were used to characterize the Cr species after calcination of the samples and FT-IR technique after reduction and adsorption of CO and C_2H_4, to investigate the active sites of chromium.

2. Experimental

2.1. Preparation of the catalysts

Cr/SiO_2 catalysts containing 0.5, 1 and 3 wt.% Cr were prepared by wetness impregnation using chromium(II) acetate (Aldrich, 99%) and bis(triphenylsilyl)chromate as precursor salts on a commercial silica gel (Davison 955, 299 m^2/g and 1.65 cm^3/g). After stirring for 18 h, in water for the acetate and *n*-hexane for the bis(triphenylsilyl)chromate, the catalysts were dried at 353 K under vacuum and calcined in dry air flow at 773 K for 30 min. Table 1 summarizes the catalysts: chromium contents, precursor salts and sample codes. Bis(triphenylsilyl)chromate was prepared by using chromium trioxide and triphenylsilanol and purified with carbon tetrachloride, following the procedure described by Carrick et al. [14].

2.2. Characterizations

The analyses of temperature programmed reduction (TPR) were accomplished in an equipment with thermal conductivity detector (TCD). The catalysts (0.5 g) were dried under argon flow at 773 K for 1 h and reduced up to 1073 K with 1.6 wt.% H_2/Ar flow (30 ml/min). The analyses of diffuse reflectance spectroscopy (DRS) were carried out in a Varian Cary 5 spectrometer in the 200 to 800 nm range (UV-VIS). The reference for the experiments was the support of the catalysts. The standards Cr_2O_3 and CrO_3 (Aldrich) were also analyzed by DRS and TPR.

Infrared spectroscopy experiments were performed on a FT-IR Perkin-Elmer 2000 spectrometer with a resolution of 4 cm^{-1}. Self supported wafers (~10 mg/cm^2) were pretreated in situ in a cell equipped with CaF_2 window. Pretreatment followed

Table 1
Chromium contents, sample codes and TPR results of the catalysts

Catalysts	Precursor salt	Cr (wt.%)	H_2 consumption (μmols H_2/mg Cr)	Cr^{x+} [a]	T (K)[b]
1CrA	Acetate	0.85	30.1	6.0	769
3CrA	Acetate	3.02	26.3	5.7	649
0.5CrB	Silyl chromate	0.56	22.0	5.3	752

[a] x: average chromium oxidation state after calcination.
[b] Temperature of the maximum H_2 consumption.

the sequence: dry under N_2 flow at 773 K for 1 h, reduction with 300 Torr CO for 30 min at 623 K and then evacuation at 10^{-5} Torr at 773 K for 1 h. After that, CO chemisorption was performed at room temperature. FT-IR spectra of the samples after reduction were obtained rationing the experimental spectra by the spectra of the dried samples. Similarly, the CO chemisorbed spectra were obtained rationing the experimental spectra by the spectra of the reduced samples.

Polymerization studies were performed at room temperature, by adding a small pulse of ethylene (5 Torr) to the reduced sample. Twelve sequences of 5 scans were obtained in the first 10 min, immediately after ethylene addition and two more 5 scans after the following 20 and 30 min. The single beam spectra just obtained were rationed against the spectra of the reduced sample in order to provide the final spectra.

3. Results and discussion

Chromium contents, determined by atomic absorption spectroscopy and the sample codes are reported in Table 1. The impregnation of organochromium salts followed by calcination had the aim to get well-dispersed chromium over the support, as reported in other catalytic systems [15]. The results of thermogravimetric analyses showed that the decomposition of both precursor salts was complete in the calcination. The catalysts from acetate showed an homogeneous yellow color after calcination, which is ascribed to Cr^{6+} ions.

The analyses of TPR (temperature programmed reduction) of the CrO_3 resulted in a single reduction peak, corresponding to 28.9 μmols H_2/mg Cr, ascribed to the complete reduction of CrO_3 to Cr_2O_3, while the Cr_2O_3 did not reduce. Diffuse reflectance spectroscopy (DRS) analyses of the catalysts after TPR showed characteristic bands of Cr_2O_3 at 272, 355, 467 and 610 nm in the 200–800 nm range (UV-VIS). These results evidenced that the final oxidation state of chromium was 3+, as reported elsewhere [16,17].

Considering that the consumption of H_2 corresponds to the complete reduction of CrO_3 to Cr_2O_3, the average oxidation state of chromium on the calcined catalysts was determined (Table 1). It turns out that the catalysts from the acetate precursor presented prevailing Cr^{6+} ions while 0.5CrB catalyst, from bis(triphenylsilyl)chromate, also presented a fraction of Cr^{3+} ions, as Cr_2O_3, after calcination, resulting the lowest average oxidation state. These attributions were also observed in the DRS analyses. The 1CrA and 3CrA presented bands at 278 and 358 nm ascribed to CrO_3, while catalyst 0.5CrB also presented small bands at 467 and 609 nm reported as Cr_2O_3 [18,19].

As showed in Fig. 1, the reduction profiles were distinct with chromium contents and precursor salts. The 1CrA and 0.5CrB catalysts showed only one reduction peak with maximum H_2 consumption at 769 and 752 K, respectively, while the 3CrA catalyst showed two peaks, at 649 and 743 K. The peak at 649 K can be ascribed to large Cr^{6+} particles, probably formed because the amount of hydroxyls groups was not sufficient to stabilize all the chromium on the silica surface.

FT-IR spectra of the reduced samples in the hydroxyls region (3800–3400 cm^{-1}) showed bands at 3747 and 3725 cm^{-1} and a broad band centered around 3600 cm^{-1}. The integration of these bands normalized by chromium loading is presented in Table 2. The band at 3747 cm^{-1} is due to isolated hydroxyls [2] and its intensity decreases as the chromium content increases, since chromium is anchored on isolated hydroxyls of silica during the preparation [20]. McDaniel [10], using a porous silica (280 m^2/g and 1.6 cm^3/g), observed a content of 2.85% Cr corresponding to a complete coverage of Cr over silica. Our results agree with McDaniel, although some residual hydroxyls could be detected on the 3CrA catalyst.

The catalysts also exhibited one band at 3600 cm^{-1}, which is ascribed to the interaction of $Cr^{2+}{}_C$ with the hydroxyls of the support [2]. The normalized integrated band presented significantly different values (Table 2). It turns out that the 1CrA catalyst presented greater amounts of $Cr^{2+}{}_C$ species than the 3CrA, which agrees with the structure of this species proposed by Kim and Woo [2], who suggested two adjacent silanol groups interacting with one Cr atom. However, the 0.5CrB catalyst presented lower $Cr^{2+}{}_C$ content than 1CrA, probably due to the presence of Cr^{3+} in the former, as suggested in the TPR results. Indeed, Cr_2O_3 was not reduced to Cr^{2+}, when a physical mixture of Cr_2O_3 (3 wt.% Cr) with silica was submitted to reduction with CO at 623 K. The catalysts also showed one band at 3725 cm^{-1},

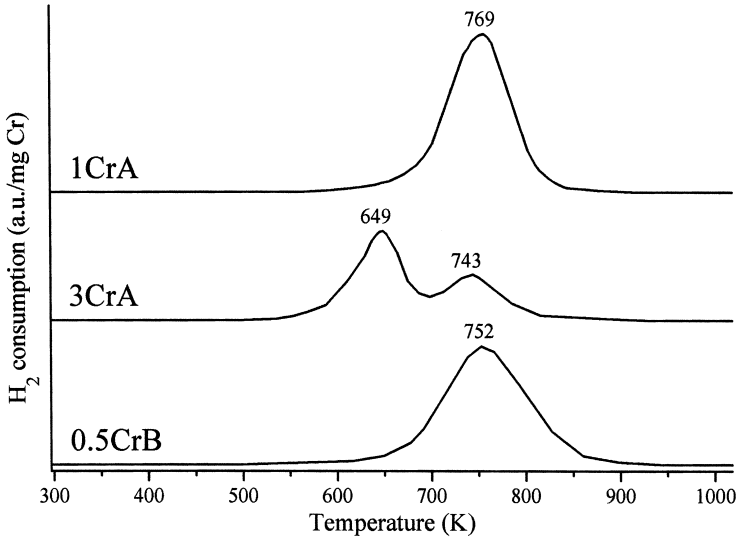

Fig. 1. TPR profiles of the catalysts.

which was related to $Cr^{2+}{}_B$, according to the literature [2]. Thus, considering that the extinction coefficients for Cr^{2+} species are equal, the ratio of the integrated areas $Cr^{2+}{}_C/Cr^{2+}{}_B$ was between 4 and 5 for the 1CrA and 0.5CrB catalysts and around 2 for the 3CrA sample. These results were supported by the relative abundance of hydroxyls at the surface of the catalysts. It evidenced that with increasing Cr content the number of free isolated hydroxyls decreased.

The infrared spectra of CO adsorbed are shown in Fig. 2. In the narrow CO adsorption region (2200–2160 cm^{-1}) only the 1CrA and 3CrA catalysts showed absorption bands. The 0.5CrB catalyst did not show any band in this region. The amount of $Cr^{2+}{}_A$ and $Cr^{2+}{}_B$ species in this catalyst is probably small to be detected by FT-IR in the CO adsorption region. This assumption is supported by the presence of a fraction of Cr_2O_3 and the relative high concentration of $Cr^{2+}{}_C$, in comparison with $Cr^{2+}{}_B$. For the 1CrA and 3CrA catalysts, the use of a computational Gaussian deconvolution resulted in two bands at 2180 and 2188 cm^{-1}, which were ascribed to CO bonded to $Cr^{2+}{}_A$ and $Cr^{2+}{}_B$ species, respectively [2]. The total intensity band of the CO chemisorption on 3CrA was more pronounced than on 1CrA.

From the FT-IR results it was possible to evaluate the distribution of Cr^{2+} species, as defined by a linear combination of the species $Cr^{2+}{}_A$, $Cr^{2+}{}_B$ and $Cr^{2+}{}_C$. It was obtained calculating the $Cr^{2+}{}_B/Cr^{2+}{}_A$ ratio from the CO adsorbed bands and $Cr^{2+}{}_C/Cr^{2+}{}_B$ from the hydroxyls band region (Table 2). Considering that the extinction coefficients are equal for all Cr^{2+} species, the relative percentage of $Cr^{2+}{}_A$, $Cr^{2+}{}_B$ and $Cr^{2+}{}_C$ are presented in Table 3. The amount of $Cr^{2+}{}_B$ species was more abundant than $Cr^{2+}{}_A$ in both

Table 2
Integrated area of FT-IR spectra bands of reduced catalysts and CO chemisorption

Catalysts	Hydroxyls region (cm mg Cr)$^{-1}$			CO region (cm mg Cr)$^{-1}$	
	3747 (OH)	3725 ($Cr^{2+}{}_B$)	3600 ($Cr^{2+}{}_C$)	2180 ($Cr^{2+}{}_A$)	2188 ($Cr^{2+}{}_B$)
0.5CrB	2.27	1.54	8.06	–	–
1CrA	2.49	5.69	20.30	0.172	0.304
3CrA	0.41	3.64	5.99	0.123	0.421

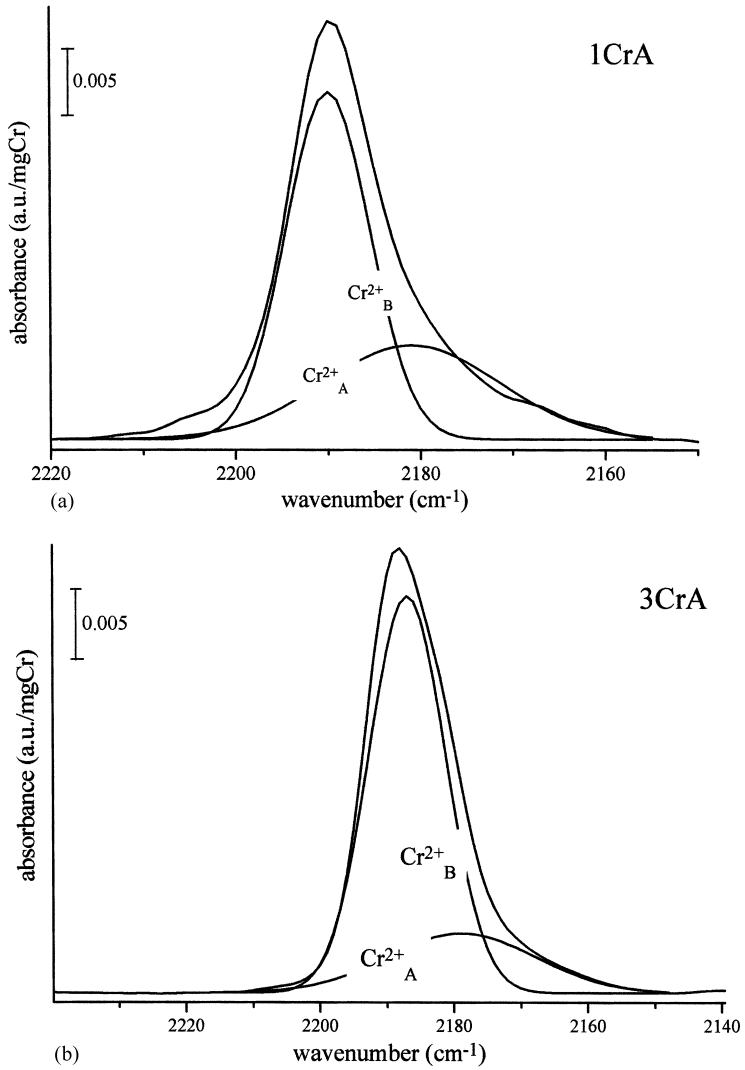

Fig. 2. FT-IR spectra of CO chemisorption on the reduced catalysts (a) 1CrA (b) 3CrA.

catalysts, 1CrA and 3CrA. The fraction of active sites $Cr^{2+}{}_A + Cr^{2+}{}_B$ was determined, being the higher value for the 3CrA catalyst. This result suggests that the 3CrA catalyst may be more active in the polymerization than 1CrA.

Table 3
Distribution of Cr^{2+} species by FT-IR experiments

Catalyst	Cr^{2+} species distribution (%)			
	$Cr^{2+}{}_A$	$Cr^{2+}{}_B$	$Cr^{2+}{}_C$	$(Cr^{2+}{}_A + Cr^{2+}{}_B)$
1CrA	11.0	19.5	69.5	30.5
3CrA	9.9	34.0	56.1	43.9

In our FT-IR procedure, a treatment of vacuum at 773 K was carried out after reduction in order to remove residual carbon monoxide. In earlier studies, Garrone et al. [3–5] used mild temperatures between 423 and 623 K, probably to avoid the conversion of $Cr^{2+}{}_A$ species into $Cr^{2+}{}_C$. That means, it is possible that a fraction of $Cr^{2+}{}_A$ was converted into $Cr^{2+}{}_C$ under vacuum after the reduction. Thus, changes in the pre-treatment

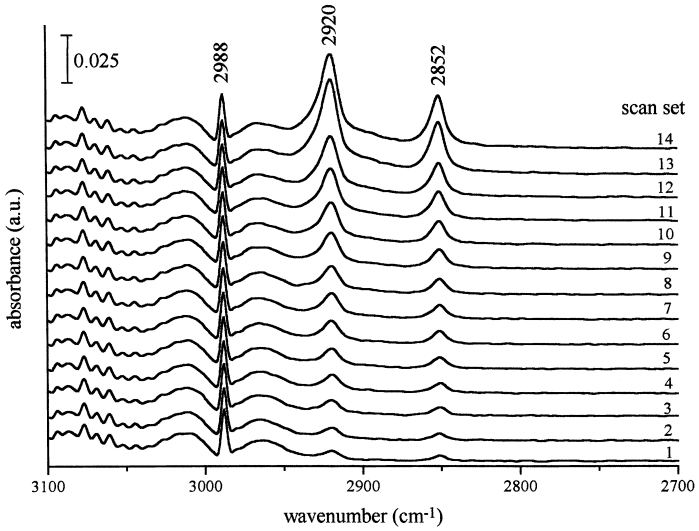

Fig. 3. FT-IR spectra of ethylene polymerization in the 1CrA catalyst at 298 K (3100–2700 cm^{-1}).

can result better performance in the polymerization.

FT-IR experiments of adsorbed ethylene were also performed after CO reduction, following evacuation at 773 K, since residual CO should inhibit ethylene polymerization on Cr/SiO_2 [21]. Each experiment was obtained with twelve groups of 5 scans, immediately after ethylene uptake, during the first 10 min. The 13th and 14th scans were obtained after 20 and 30 min, respectively. The 1CrA and 3CrA catalysts exhibited three main bands, as shown in Figs. 3 and 4, respectively. The band at 2988 cm^{-1} can be ascribed to $\upsilon_s(CH_2)$ of ethylene π-adsorbed on Cr^{2+} sites [11–13], although Sheppard and Yates [22] suggested that this band occurs at 2980 cm^{-1}. The other two bands, at 2920 and 2852 cm^{-1}, correspond to

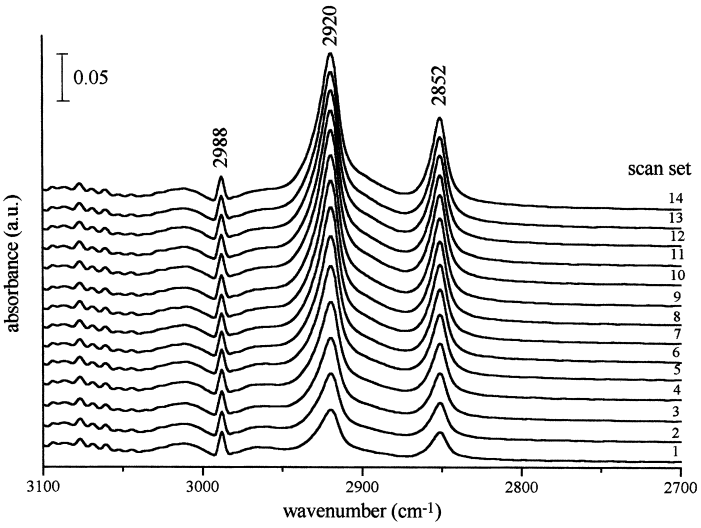

Fig. 4. FT-IR spectra of ethylene polymerization in the 3CrA catalyst at 298 K (3100–2700 cm^{-1}).

Table 4
Integrated area of ethylene FT-IR spectra bands

Catalyst	Ethylene bands (cm mg Cr)$^{-1}$ [a]	
	2988	2920
0.5CrB	0.81	0.096
1CrA	0.41	4.30
3CrA	0.14	5.31

[a] 30 min of reaction.

$\upsilon_{as}(CH_2)$ and $\upsilon_s(CH_2)$ of the polymer chain. The band at 2988 cm^{-1} practically did not change during the analyses for all catalysts. The 0.5CrB catalyst showed the band at 2988 cm^{-1} and another very small band at 2920 cm^{-1}, which did not change significantly during the analyses. However, the band at 2852 cm^{-1} was not detected for this catalyst. These results are coherent with low concentration of active species, since no adsorption of CO was observed for the 0.5CrB catalyst.

The FT-IR spectra of 1CrA and 3CrA in the 1500–1350 cm^{-1} region showed three bands at 1445, 1465 and 1470 cm^{-1}. The first one was attributed to ethylene π-adsorbed on Cr^{2+} sites, that also remained constant during the analyses as observed for the band at 2988 cm^{-1}. The bands at 1465 and 1470 cm^{-1} were ascribed to bending modes of methylene groups of polyethylene [11–13]. Indeed, these bands increased, following the same behavior of the 2920 and 2855 cm^{-1} bands.

Table 4 presents the integrated areas of the 2988 and 2920 cm^{-1} bands of ethylene polymerization after 30 min of reaction (14th spectrum). From the 2988 cm^{-1} band, it turned out that the 0.5CrB catalyst exhibited greater amount of ethylene π-adsorbed than the other two catalysts. On the other hand, it was inversely proportional to the activity: the activity was lower with more π-adsorbed ethylene on Cr^{2+} sites. This behavior suggests the existence of two types of Cr^{2+} sites: one which is active for the polymerization and other one that just adsorbs ethylene [12]. Therefore, the $Cr^{2+}{}_C$ species could be classified in the second case whereas the $Cr^{2+}{}_A$ and $Cr^{2+}{}_B$ species in the first case, according to the distribution of these species in the catalysts. Following the 2920 cm^{-1} band, which was ascribed to a polymer chain growth, the 3CrA catalyst presented the highest value of the integrated area, and therefore, a better activity than the 1CrA and 0.5CrB samples, as shown in Table 4.

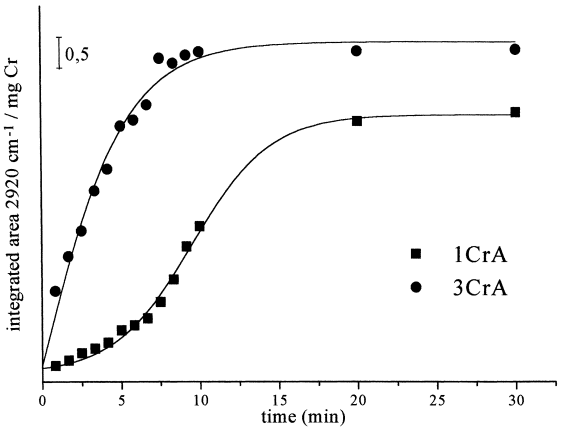

Fig. 5. Ethylene polymerization at 298 K vs. time for the catalysts.

Fig. 5 presents the behavior of the polyethylene (-CH_2-) band at 2920 cm^{-1} with time. An initial polymer absorbance was noted just at the beginning of the experiment on both samples. Without induction time, the 1CrA catalyst showed low initial activity. Polymerization stopped after reaching 10 min on 3CrA and 20 min on 1CrA. There are two main suggestions that could explain this behavior: the first one is that the polymerization proceeded on active Cr^{2+} sites just at the beginning, as observed in the FT-IR analyses, but then the polymer blocked the access to the other sites, interrupting the reaction. The second explanation is the possible presence of poisons in the ethylene feed, such as oxygen or water.

The differences in polymerization activity on both catalysts should not be attributed entirely to the presence of the $Cr^{2+}{}_A$ species, since 1CrA and 3CrA exhibited almost the same fraction of this species (Table 3). Probably, there is a contribution of the $Cr^{2+}{}_A$ and $Cr^{2+}{}_B$ species. Indeed, the 3CrA catalyst presented approximately 1.4 times more $Cr^{2+}{}_A$ and $Cr^{2+}{}_B$ species than 1CrA (Table 3), which agreed with the change of the integrated absorbance of 2920 cm^{-1} band of ethylene polymerization (Table 4). According to the literature, $Cr^{2+}{}_A$ is the most reactive species in the polymerization, but $Cr^{2+}{}_B$ or mixed species of $Cr^{2+}{}_A$ and $Cr^{2+}{}_B$ are not discarded [3,4,6].

Finally, Fig. 6 presents the behavior of isolated hydroxyls during the polymerization reaction, by

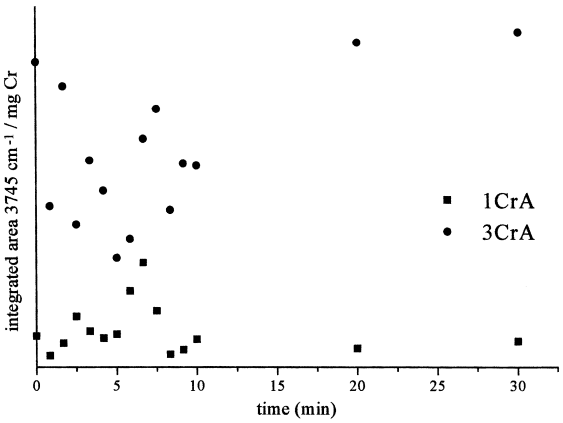

Fig. 6. Behavior of isolated hydroxyls band (3745 cm^{-1}) during polymerization.

integration of the band at 3745 cm^{-1}. This band was not shifted to 3696 cm^{-1}, which was ascribed to the interaction of surface hydroxyls with the polymer chain [9,13]. The band at 3745 cm^{-1} showed a random behavior, whereas Jozwiak et al. [7] observed linearity. Besides, the amounts of isolated hydroxyls before and at the end of the polymerization growth were similar, suggesting that the hydroxyls contributed to the polymerization mechanism, in agreement with the reaction mechanisms proposed by Jozwiak et al. [7] and Groeneveld et al. [8].

4. Conclusions

FT-IR spectroscopy analyses allow to characterize the three Cr^{2+} species ($Cr^{2+}{}_A$, $Cr^{2+}{}_B$ and $Cr^{2+}{}_C$) in Cr/SiO_2 catalysts and their different behaviors in the ethylene polymerization. The chromium content, which influenced the amount of surface hydroxyls and the precursor salt affected largely the Cr^{2+} species distribution. Different activities of ethylene polymerization was observed on two catalysts with similar $Cr^{2+}{}_A$ content. The 3CrA catalyst presented the greatest amount of $Cr^{2+}{}_A$+$Cr^{2+}{}_B$ species and the best activity. Our results suggested that not only $Cr^{2+}{}_A$, but also $Cr^{2+}{}_B$ or a mixed $Cr^{2+}{}_A + Cr^{2+}{}_B$ sites have activity in the polymerization. The behavior of isolated hydroxyls band during the polymerization suggests its participation in the reaction mechanism.

References

[1] B.M. Weckhuysen, R.A. Schoonheydt, Catal. Today 51 (1999) 215.
[2] C.S. Kim, S.I. Woo, J. Mol. Catal. 73 (1992) 249.
[3] A. Zecchina, G. Spoto, G. Ghiotti, E. Garrone, J. Mol. Catal. 86 (1994) 423.
[4] E. Garrone, G. Ghiotti, A. Zecchina, in: Y. Imamoglu (Ed.), Olefin Metathesis and Polymerization Catalysts, Kluwer Academic Publishers, Amsterdam, 1990, p. 393.
[5] B. Fubini, G. Ghiotti, L. Stradella, E. Garrone, C. Morterra, J. Catal. 66 (1980) 200.
[6] G. Ghiotti, E. Garrone, A. Zecchina, J. Mol. Catal. 46 (1988) 61.
[7] W.K. Jozwiak, I.G. Dalla Lana, R. Fiedorow, J. Catal. 121 (1990) 183.
[8] C. Groeneveld, P.P.M.M. Wittgen, H.P. Swinnen, A. Wernsen, C.G.A. Schuit, J. Catal. 83 (1983) 346.
[9] M.P. McDaniel, M.B. Welch, J. Catal. 82 (1983) 98.
[10] M.P. McDaniel, Adv. Catal. 33 (1985) 47.
[11] M. Kantcheva, I.G. Dalla Lana, J.A. Szymura, J. Catal. 154 (1995) 329.
[12] K. Vikulov, G. Spoto, S. Coluccia, A. Zecchina, Catal. Lett. 16 (1992) 117.
[13] O.M. Bade, R. Blom, I.M. Dahl, A. Karlsson, J. Catal. 173 (1998) 460.
[14] W.L. Carrick, R.J. Turbett, F.J. Karol, G.L. Karapinka, A.S. Fox, R.N. Johnson, J. Pol. Sci. A-1 10 (1972) 2609.
[15] J.P. Boitiaux, J. Cosyns, S. Vasudevan, in: G. Poncelet, P. Grange, P.A. Jacobs (Eds.), Preparation of Catalysts III, Elsevier, Amsterdam, 1983, p. 123.
[16] W. Hill, G. Öhlmann, J. Catal. 123 (1990) 147.
[17] B. Parlitz, W. Hanke, R. Fricke, M. Richter, U. Roost, G. Öhlmann, J. Catal. 94 (1985) 24.
[18] B.M. Weckhuysen, L.M. De Ridder, R.M. Schoonheydt, J. Phys. Chem. 97 (1993) 4756.
[19] B.M. Weckhuysen, A.A. Verberckmoes, A.R. De Baets, R.A. Schoonheydt, J. Catal. 166 (1997) 160.
[20] M.A. Vuurman, I.E. Wachs, D.J. Stufkens, A. Oskam, J. Mol. Catal. 80 (1993) 209.
[21] M.P. McDaniel, S.J. Martin, J. Phys. Chem. 95 (1991) 117.
[22] N. Sheppard, D.J.C. Yates, Proc. Roy. Soc. A238 (1956) 69.